nature geoscience

SUPPLEMENTARY INFORMATION

DOI: 10.1038/NGEO1601

Direct Measurement of Hydroxyl in the Lunar Regolith and the Origin of Lunar Surface Water

Yang Liu[1*], Yunbin Guan[2], Youxue Zhang[3], George R. Rossman[2], John M. Eiler[2], and Lawrence A. Taylor[1]

[1]Planetary Geosciences Institute, Department of Earth & Planetary Sciences, University of Tennessee, Knoxville, TN 37996.
[2]Division of Geological and Planetary Sciences, California Institute of Technology, Pasadena, CA 91125.
[3]Department of Earth and Environmental Sciences, University of Michigan, Ann Arbor, MI 48109.

Supplementary Information

1. Samples

Agglutinates were picked from three soil samples. Apollo 11 soil 10084 is a mature soil, whereas Apollo 16 soil 64501 is a sub-mature one. Sample 70051 was collected from the surface of the lunar rover at the conclusion of the Apollo 17 mission, and is considered to be immature[1].

2. Analytical methods

All reported FTIR data were collected using a microscope of a Perkin-Elmer Spectrum FTIR GX at the University of Michigan. Transmitted IR spectra were collected using a visible source, a CaF_2 beamsplitter, a liquid-N_2 cooled MCT detector, a rectangle aperture (100 by 80-100 μm), 512 scans, resolution of 4 cm^{-1}, and a gain of 1 to 4. To minimize the interference of atmospheric H_2O, samples were shielded in a compartment purged with a constant N_2 flow, and a new background scan was collected just before the sample scan. The total H_2O contents were

estimated following the Beer-Lambert law: $c = 18.02 \times Abs/(d \times \rho \times \varepsilon)$, where *Abs* is the absorbance at ~3480 cm^{-1} (peak value) corrected for the baseline, *d* is the thickness of the sample, ε is the molar absorption coefficient and is 61 *l*/mol/cm for the basaltic glass[2], ρ is the density of the glass assuming a constant value of 3000 kg/m^3. The ε values differ by <6% among different basalts[3]. Detection limit of the FTIR spectrometer is ~10 ppmw H_2O. However, owing to the small size of the peak at ~3500 cm^{-1} and the uncertainty in sample thickness and in the baseline fitting, the estimated OH contents are much larger (20 to 30%).

Back scattered electron (BSE) images and the composition of the glasses and minerals were acquired using a Cameca SX-100 electron microprobe (EMP) at the University of Tennessee. Analytical conditions include a voltage of 15 KeV, a current of 10 nA, and a 10 μm beam diameter. Natural and synthetic minerals are used as standards. Detection limits are typically <0.05 wt% for SiO_2, Al_2O_3, MgO, CaO, Na_2O and K_2O; 0.06-0.1 wt% for FeO, TiO_2, Cr_2O_3, MnO, P_2O_5 and S. Major and minor element contents of glass and minerals are shown in Supplementary Table 1 and Supplementary Figure 1.

Analyses for H abundances and D/H values were conducted in two sessions with a Cameca ims-7f GEO ion probe at Caltech. For both sessions, the areas of interest were examined carefully using ion imaging to avoid C and H hotspots (cracks, vesicles). Spots chosen for SIMS analyses are near EMP points. Following a ~3 min sputtering, glassy regions were measured for 20 cycles through the mass sequence of $^{12}C^-$, $^{16}O^1H^-$, [$^{18}O^-$], $^{12}C^{16}N^-$, $^{30}Si^-$, [$^{31}P^-$], $^{32}S^-$, and $^{35}Cl^-$, where the masses in brackets were only measured in the second session. A mass resolving power (ΔM/M) of 5500 was used to separate the $^{16}O^1H$ peak from ^{17}O. Terrestrial basaltic glasses with 150 and 260 ppmw H_2O[4] were used as standards for H abundances (Supplementary Figure 2). Supplementary Figure 3 shows an example of the SIMS spectra for OH

measurements. The instrument H backgrounds of the two sessions were monitored with a dry olivine standard (GRR1017, <<1 ppmw H_2O[5]). The background $^{16}O^{1}H^{-}/^{30}Si^{-}$ values were subtracted from those of standards and samples. Using the method in Mosenfelder et al.[5], the detection limit of SIMS is estimated to be 7 and 5 ppmw H_2O for two sessions, respectively. The uncertainties (2σ in Supplementary Table 1) of the OH measurements were estimated based on the external errors of the standards (repeated measurements of the standards, the errors associated with them, both in their slopes and intercepts) and the internal errors.

D/H measurements were conducted on the same spots where H abundances were obtained. The mass sequence of $^{1}H^{-}$, $^{2}H^{-}$, and $^{16}O^{-}$ was measured for 15-20 cycles each with 1 s, 15 s and 1 s counting times. One terrestrial rhyolitic glass containing 0.69 wt% H_2O with $\delta D = -69‰_{VSMOW}$ (MC84-df[6]) was used to evaluate the instrument mass fractionation (IMF) of D/H. Given the small OH contents, the matrix effect between basaltic and rhyolitic glasses[7] is insignificant for the results presented in this study. The analyses of the rhyolitic glass yielded an IMF of +30‰. All reported values were corrected for the IMF. The 2σ uncertainties (Fig. 2 and 3, Supplementary Table 1) include both external errors (two analyses of the rhyolitic standard) and internal errors (counting statistics). The analytical spots corresponding to Supplementary Table 1 are shown on the BSE images of the agglutinates (Supplementary Figure 4).

3. Calculation of spallation-generated deuterium

For this calculation, we assume hydrogen was derived from solar-wind and deuterium was generated by cosmic-ray and solar-flare spallation. Using a spallation production rate of D at the surface (1.5×10^{-12} mole D_2/g/Myr)[8], and a solar-flare exposure age of 10084 (100 Ma[9]), we obtained 6×10^{-10} g of spallation-D per gram of the regolith, similar to that estimated by

Epstein and Taylor[10]. The spallation-D (molar) was divided by measured H (molar) in each agglutinates and then compared to measured D/H values (Supplementary Figure 5). Five agglutinates lie on the 1:1 line considering the uncertainties in the calculated D/H values (Supplementary Figure 5). Three grains of Apollo 11 soil 10084 (10084agg2, 10084agg3, 10084agg8ir) appear to contain D higher than that from spallation. If D in these grains were all derived from spallation, their exposure ages would be 0.6 Ga (10084agg3), 1.3-1.5 Ga (10084agg8ir) and 14 Ga (10084agg2) assuming the same D production rate. The spallation production rate is poorly constrained. If we assume the rate is 10 times more than the estimated value, the exposure ages decrease to 60 Ma (10084agg3), 130-150 Ma (10084agg8ir), and 1.4 Ga (10084agg2). The lower end of this range is possible, but the upper end is not. Thus, either production rates of D through spallation are strongly under estimated in prior studies, or grain 10084agg2 contains D from some other source.

4. Calculation hydrogen isotope composition of vapor from volcanic degassing

At the oxygen fugacity of IW-2 to IW, the vapor contains H_2 and H_2O. Let R=D/H and x = $X_{H_{2,v}}$. Thus, for the hydrogen isotope composition of the vapor (*v*), we have:

$$R_v = (1-x) * R_{H_2O_v} + x * R_{H_{2,v}}$$

$$=(1-x) * R_{H_2O_v} + x / \alpha_{H_2O_v - H_2v} \; R_{H_2O_v}$$

$$= (1-x + x / \alpha_{H_2O_v - H_2v}) \, R_{H_2O_v}.$$

The mole fraction of H_2 in the vapor is approximated by the fugacity ratio of H_2/H_2O (10:1 at log f_{O2} = IW-2 to 1:1 at log f_{O2} = IW)[11]. The fractionation factor $\alpha_{H_2O_v - H_2v}$ is 1.0875 at 1300 °C[12]. For the melt, dissolved H_2 and molecular H_2O are insignificant compared to OH[11]. It is thus reasonable to assume there is no fractionation between H_2 in the vapor and that in the melt, and

H_2 in the melt and OH in the melt. Therefore the exchange reactions between vapor and melt follow:

$$H_2O\ (v) + HDO\ (m) = HDO\ (v) + H_2O\ (m)$$

$$H_2O\ (m) + 2\ OH\ (m) = HDO\ (m) + OH\ (m) + OD\ (m)$$

$$R_{H2Ov}/\ R_{OH,\ melt} = \alpha_{H_2O_v\ -\ H_2O_m} * \alpha_{H_2O_m\ -\ OH_m}$$

Using values for rhyolite[6], $\alpha_{H2Ov\ -\ H2Om} = 0.9857$ and $\alpha_{H_2O_m\ -\ OH_m} = 1.049$, we have $\alpha_{H_2O_v\ -\ melt} = 1.034$. Thus,

$$R_v = (1\text{-}x + x/\alpha_{H_2O_v\ -\ H_2v})\ R_{H_2O_v}$$

$$= (1\text{-}x + x/1.087)*\ R_{OH,\ melt}*1.034$$

For $\delta D_{melt} = +340$ ‰ for glass beads corrected for spallation[13], the δD_v in equilibrium with the melt is ~+284 to +330 ‰ for IW-2 to IW, respectively.

5. Supplementary references

1. Hill, E., Mellin, M. J., Deane, B., Liu, Y. & Taylor, L. A. Apollo sample 70051 and high- and low-Ti lunar soil simulants MLS-1A and JSC-1A: Implications for future lunar exploration. *J. Geophys. Res.* **112**, E02006, doi:10.1029/2006je002767 (2007).
2. Danyushevsky, L. V. *et al.* The H_2O content of basaltic glasses from Southwest Pacific back-arc basins. *Earth Planet. Sci. Lett.* **117**, 347-362 (1993).
3. Mandeville, C. W. *et al.* Determination of molar absorptivities for infrared absorption bands of H_2O in andesitic glasses. *Am. Miner.* **87**, 813-821 (2002).
4. Jochum, K. P. *et al.* MPI-DING reference glasses for in situ microanalysis: New reference values for element concentrations and isotope ratios. *Geochem. Geophys. Geosyst.* **7**, doi:10.1029/2005gc001060 (2006).

5. Mosenfelder, J. L. *et al.* Analysis of hydrogen in olivine by SIMS: Evaluation of standards and protocol. *Am. Mineral.* **96**, 1725-1741 (2011).
6. Newman, S., Epstein, S. & Stolper, E. M. Water, carbon dioxide, and hydrogen isotopes in glasses from the ca. 1340 A.D. eruption of the Mono Craters, California: Constraints on degassing phenomena and initial volatile content. *J. Volcanol. Geotherm. Res.* **35**, 75-96 (1988).
7. Hauri, E. H. *et al.* Matrix effects in hydrogen isotope analysis of silicate glasses by SIMS. *Chem. Geol.* **235**, 352-365 (2006).
8. Merlivat, L., Lelu, M., Nief, G. & Roth, E. Deuterium, hydrogen, and water content of lunar material. *Proc. 5th Lunar Sci. Conf., Suppl. 5, Geochim. Cosmochim. Acta* **2**, 1885-1895 (1974).
9. Gopalan, K., Goswami, J. N., Rao, M. N., Suthar, K. M. & Venkatesan, T. R. Solar cosmic ray produced noble gases and tracks in lunar fines 10084 and 14163. *Proc. Lunar Sci. Conf.*, **8**, 793-811 (1977).
10. Epstein, S. & Taylor, H. P. O^{18}/O^{16}, Si^{30}/Si^{28}, D/H, and C^{13}/C^{12} ratios in lunar samples. *Proc. 2nd Lunar Sci.Conf.* **2**, 1421-1441 (1971).
11. Zhang, Y. "Water" in lunar basalts: The role of molecular hydrogen (H_2), especially in the diffusion of the H component. *Lunar Planet. Sci. Conf.* **42**, 1957 (2011).
12. Richet, P., Bottinga, Y. & Javoy, M. A review of hydrogen, carbon, nitrogen, oxygen, sulphur, and chlorine stable isotope fractionation among gaseous molecules. *Ann. Rev. Earth Planet. Sci.* **5**, 65-110 (1977).
13. Saal, A. E., Hauri, E. H., Van Orman, J. A. & Rutherford, M. C. D/H ratios of the lunar volcanic glasses. *Lunar Planet. Sci. Conf.* **43**, 1327 (2012).

14. Papike, J. J., Simon, S. B. & Laul, J. C. The lunar regolith - chemistry, mineralogy, and petrology. *Rev. Geophy.* **20**, 761-826 (1982).

15. Taylor, L. A., Pieters, C. M., Keller, L. P., Morris, R. V. & McKay, D. S. Lunar mare soils: Space weathering and the major effects of surface-correlated nanophase fe. *J. Geophys. Res.* **106**, 27985-27999 (2001).

16. Taylor, L. A. *et al.* Mineralogical and chemical characterization of lunar highland soils: Insights into the space weathering of soils on airless bodies. *J. Geophys. Res.* **115**, E02002 (2010).

Supplementary Figures and Table

Supplementary Figure 1. Compositions of agglutinitic glasses in this study. Filled fields represent bulk compositions of lunar soils, and open fields show average compositions of agglutinitic glasses[14-16]. Sample 10084agg2 plots together with other agglutinates.

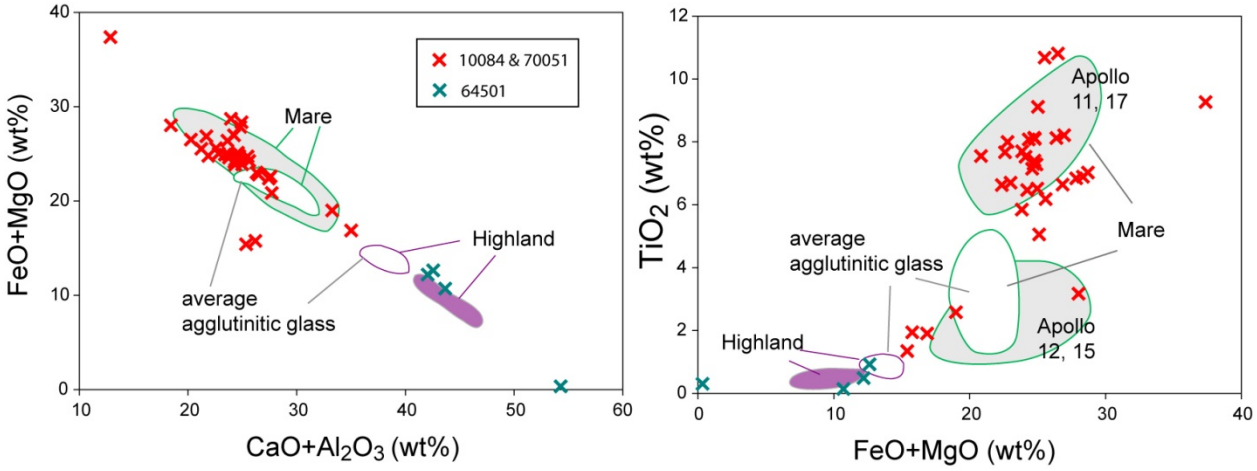

Supplementary Figure 2. Calibration lines for two analytical sessions. The $^{16}O^{1}H/^{30}Si$ values have been background corrected. The 2σ uncertainties of $^{16}O^{1}H/^{30}Si$ and H_2O content are shown if larger than the symbols. Linear regressions were conducted by weighting the $^{16}O^{1}H/^{30}Si$ and H_2O content with their 2σ uncertainties.

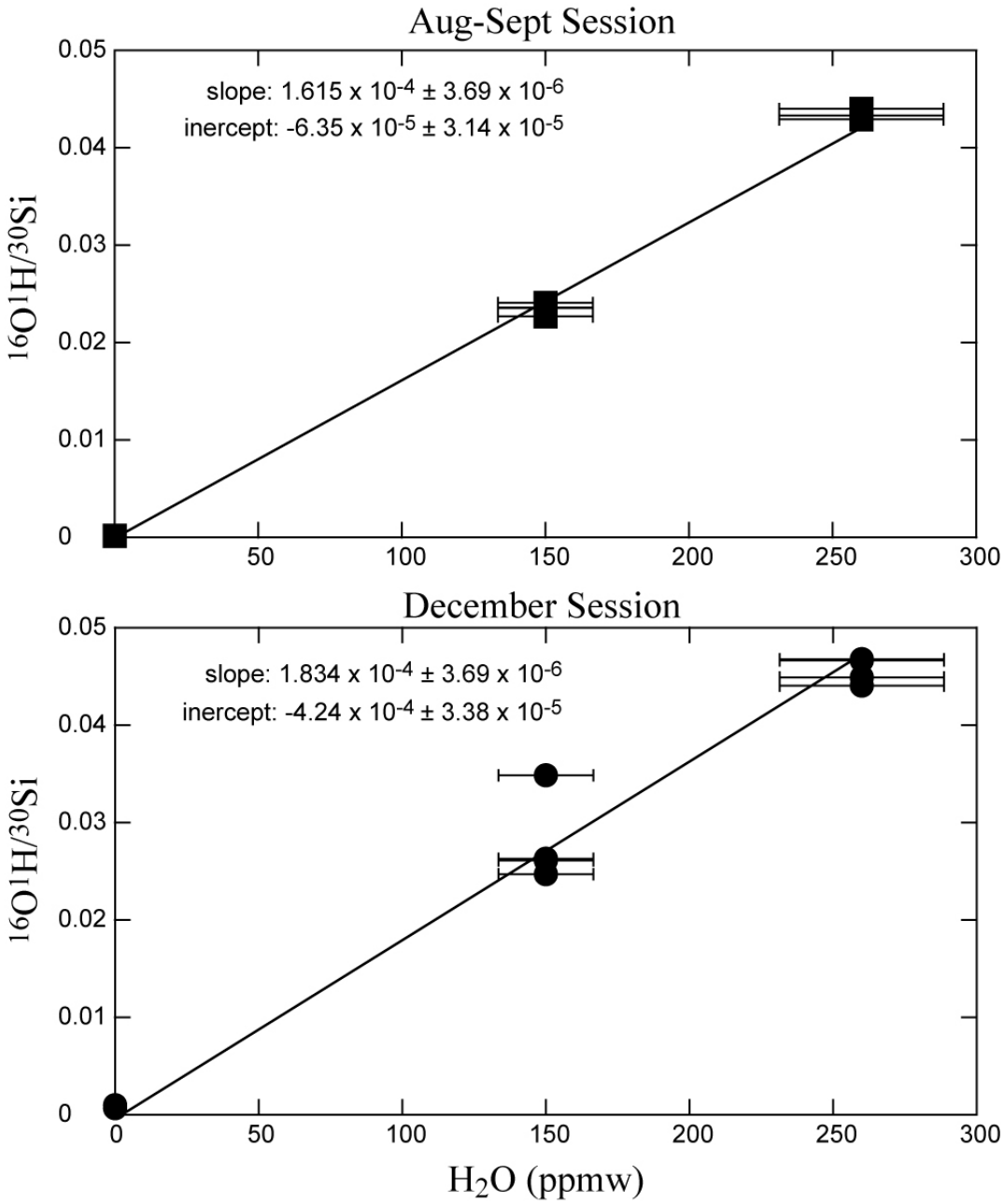

Supplementary Figure 3. SIMS spectrum for OH analysis.

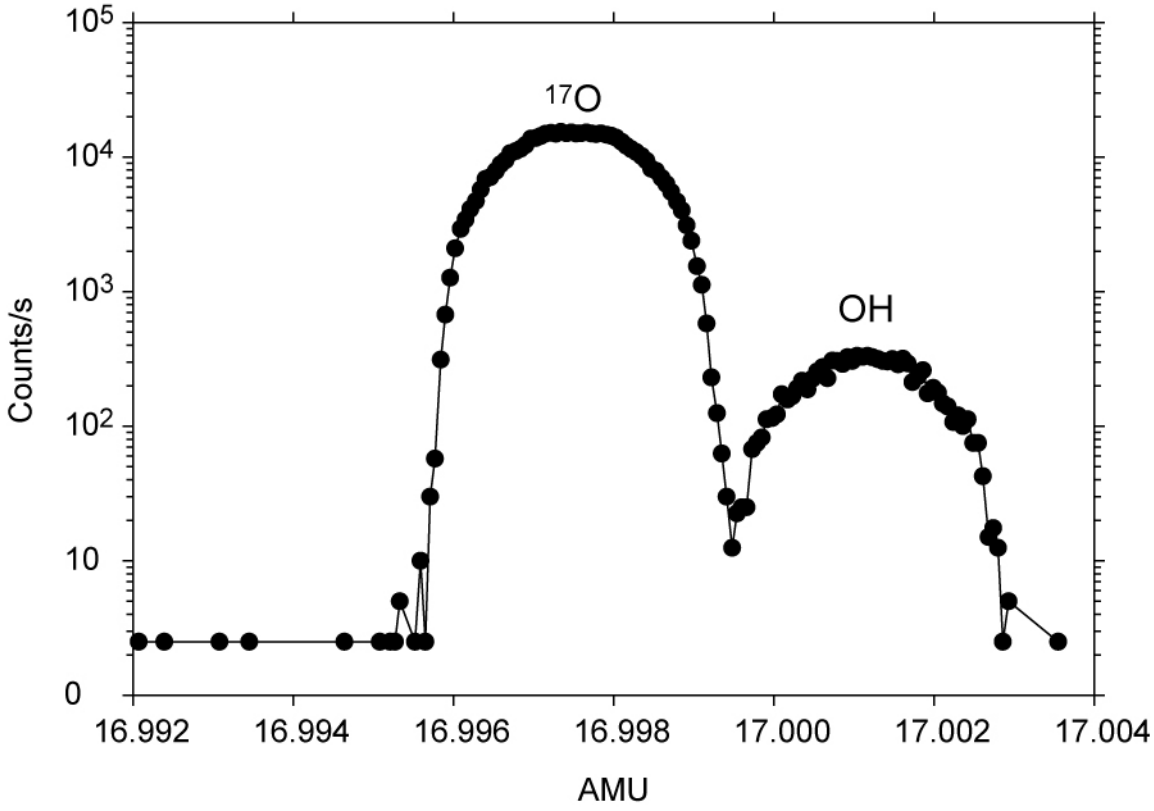

Supplementary Figure 4. Backscattered electron images of lunar agglutinates showing SIMS analytical spots. The SIMS spots for H abundances are labeled according to dates. The spots for D/H ratios are labeled with DH_###. Sample names containing 'ir' indicate that transmitted FTIR analyses had been conducted. Examples of SIMS time-lapsed spectra are plotted for two analyses.

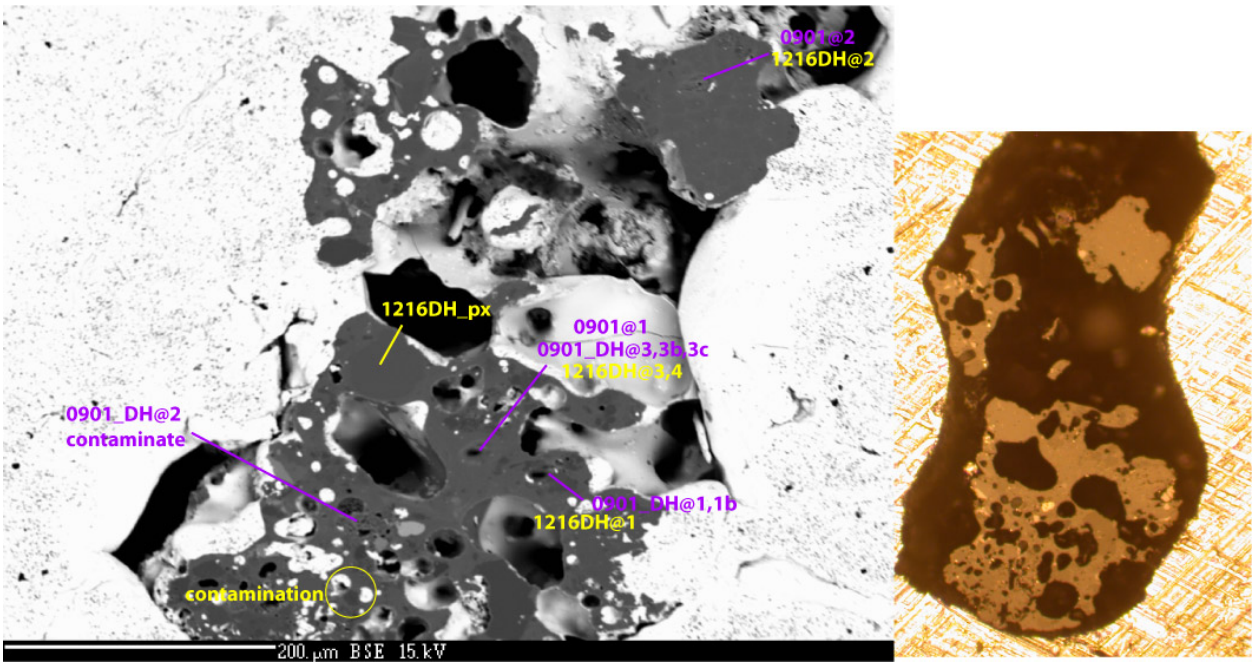

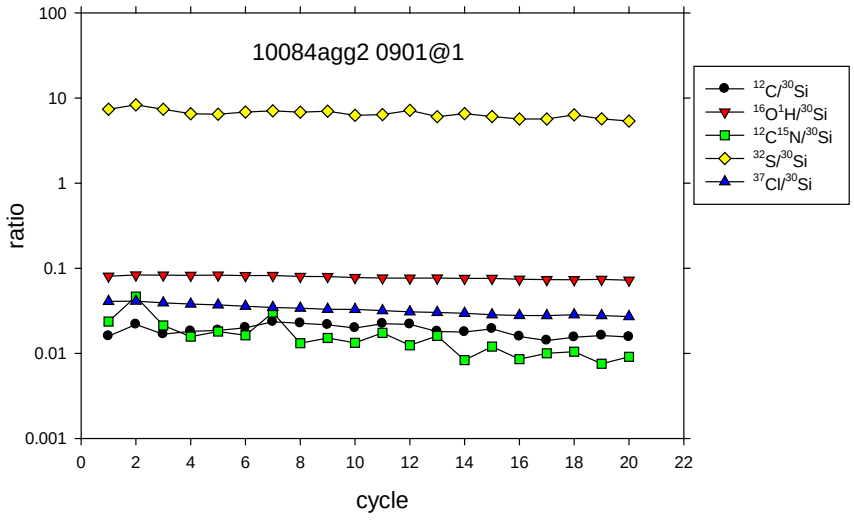

Time lapse plot for spot 0901@1

10084agg2

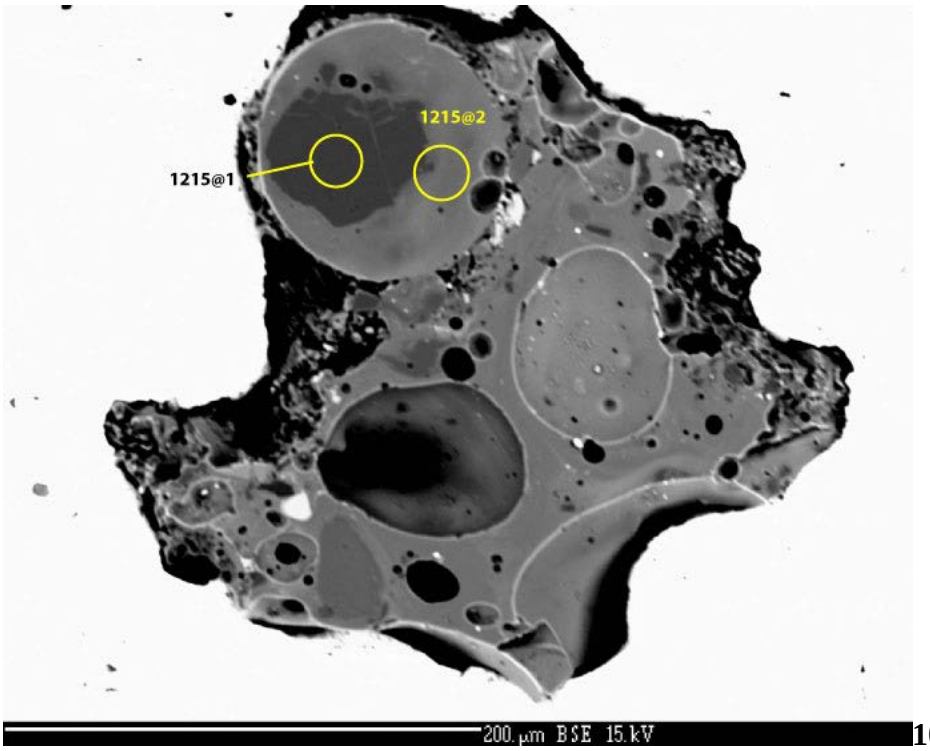

10084 agg1ir

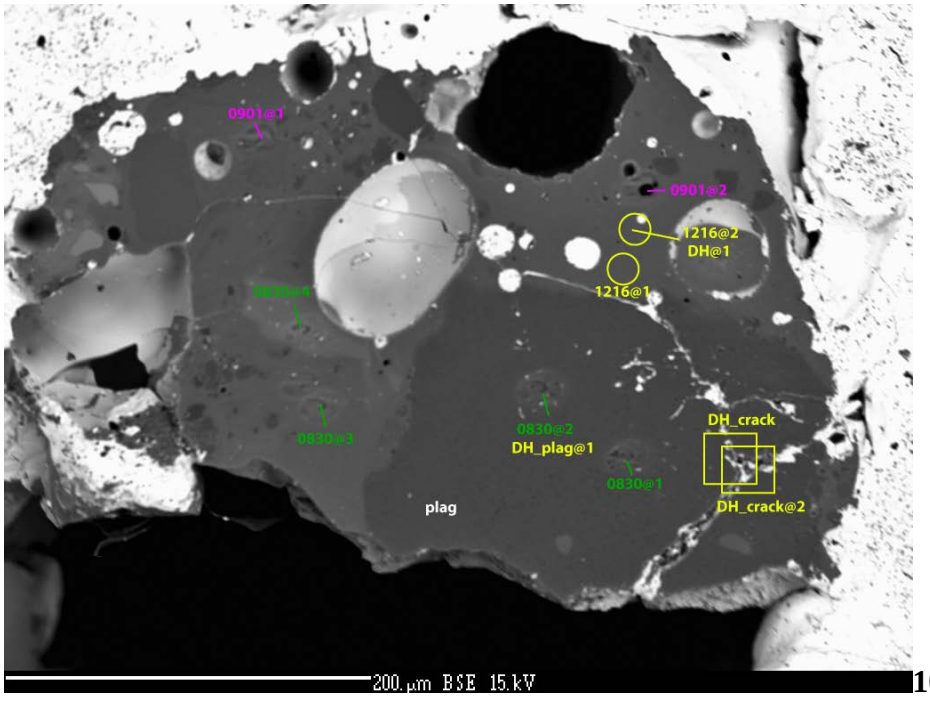

10084agg3

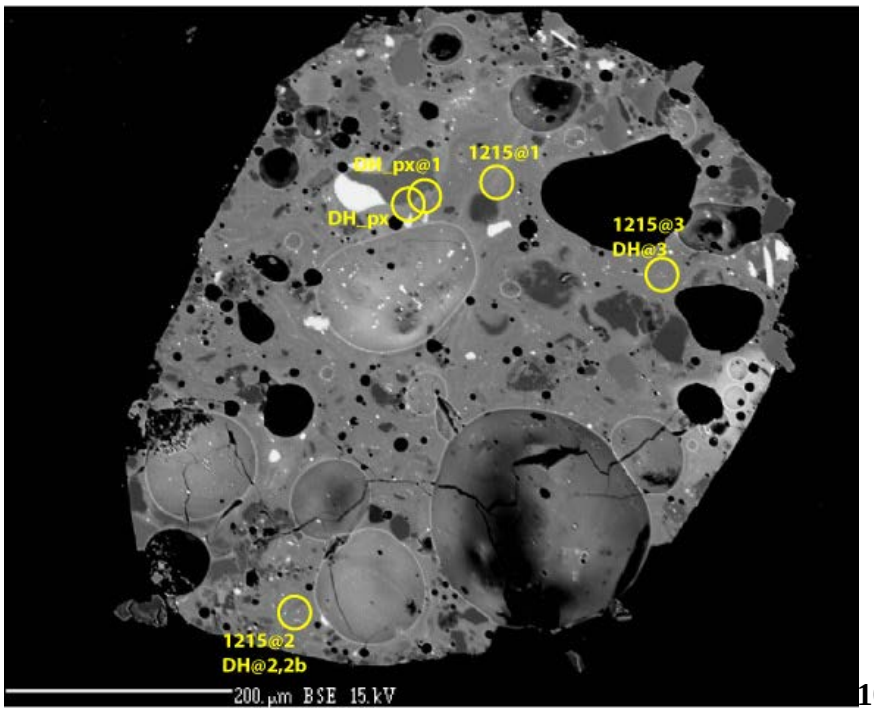

10084agg4n

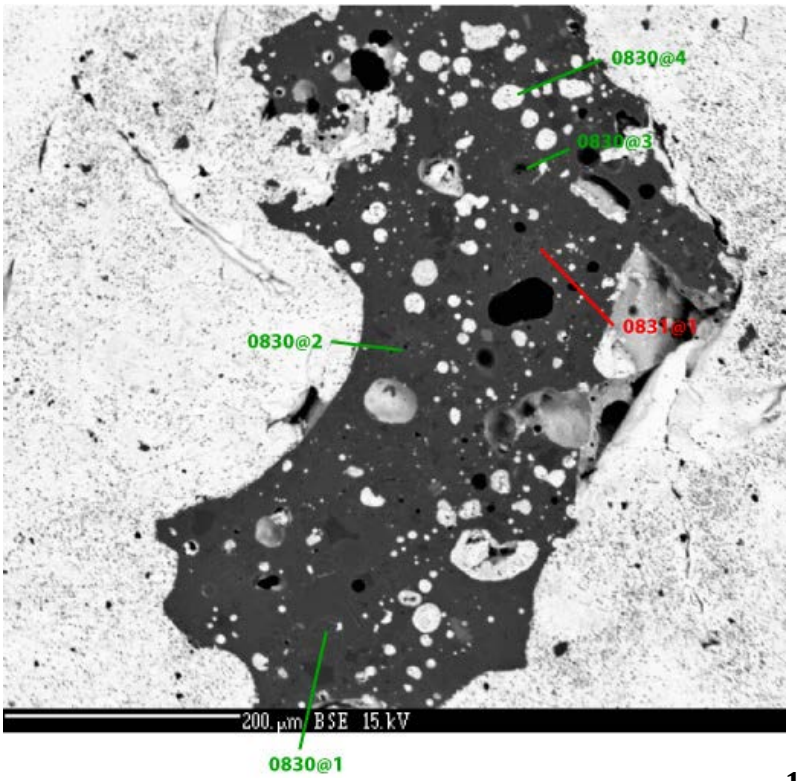

10084 agg5ir

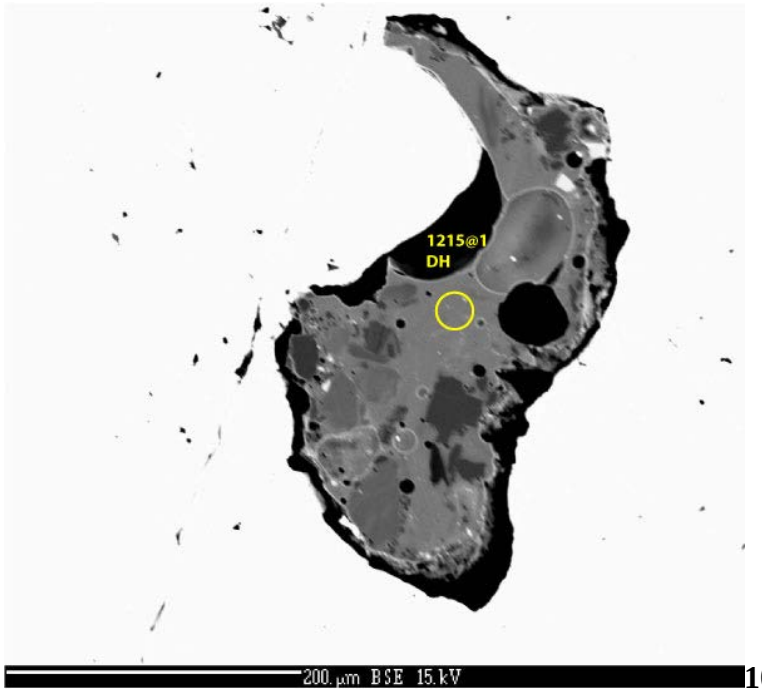

10084agg6ir

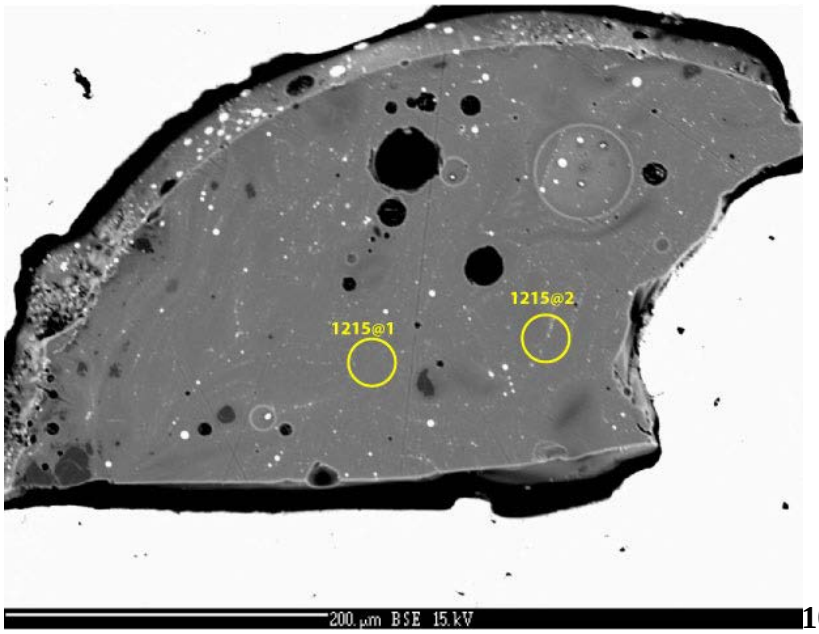

10084 agg7

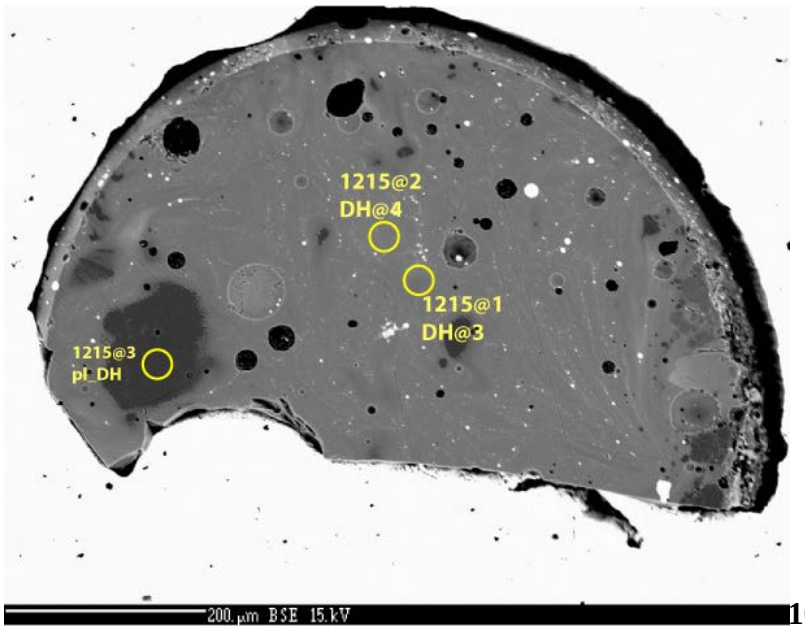

10084 agg8

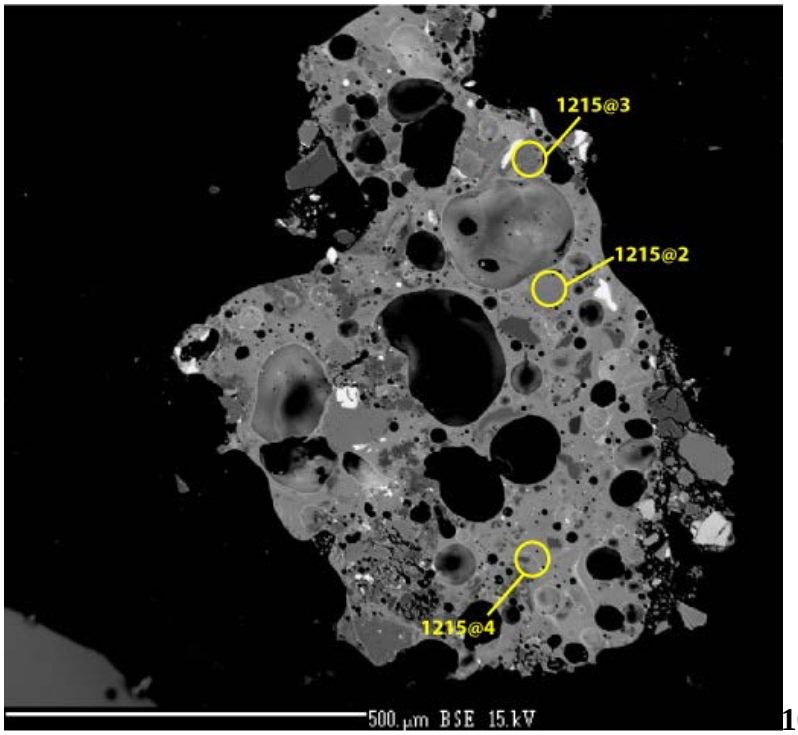

10084 agg9

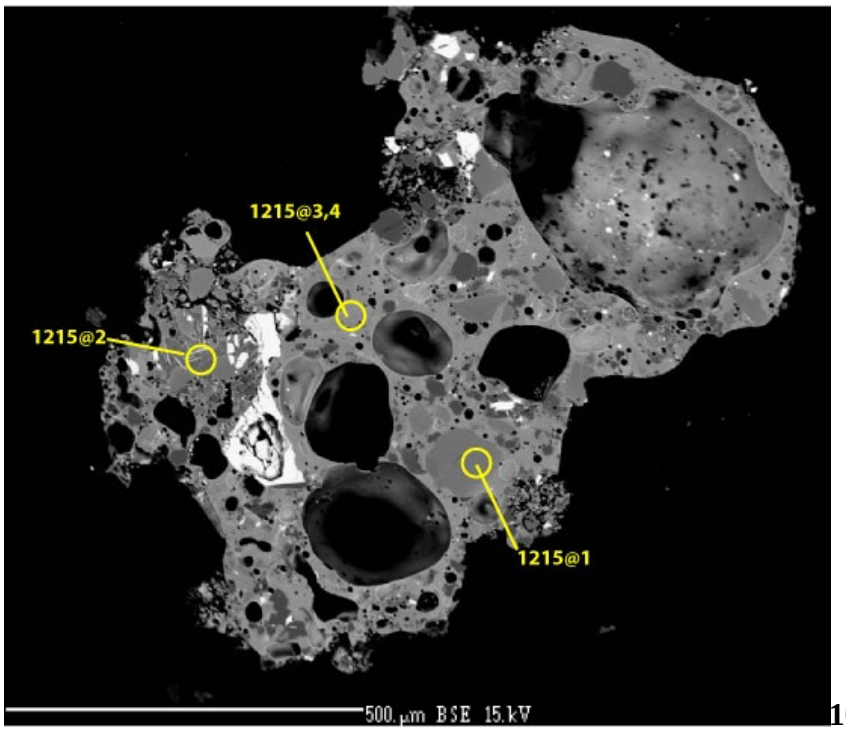

10084agg10

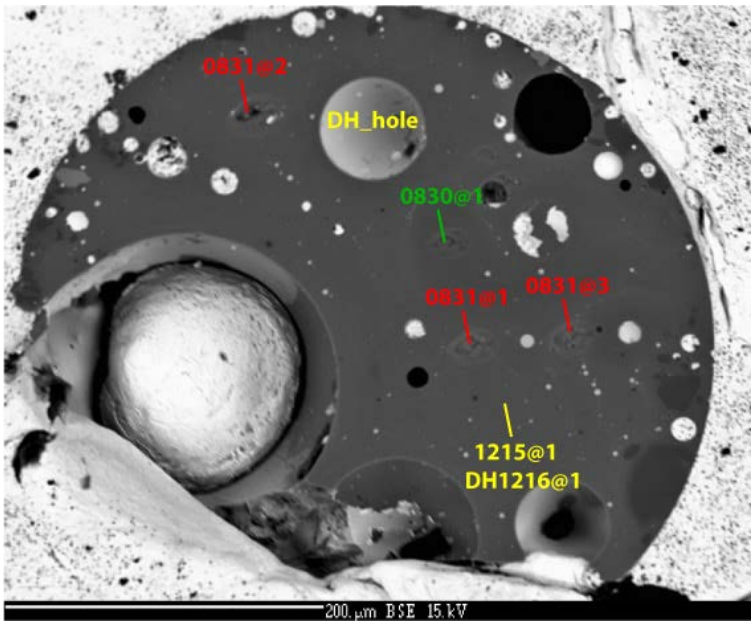

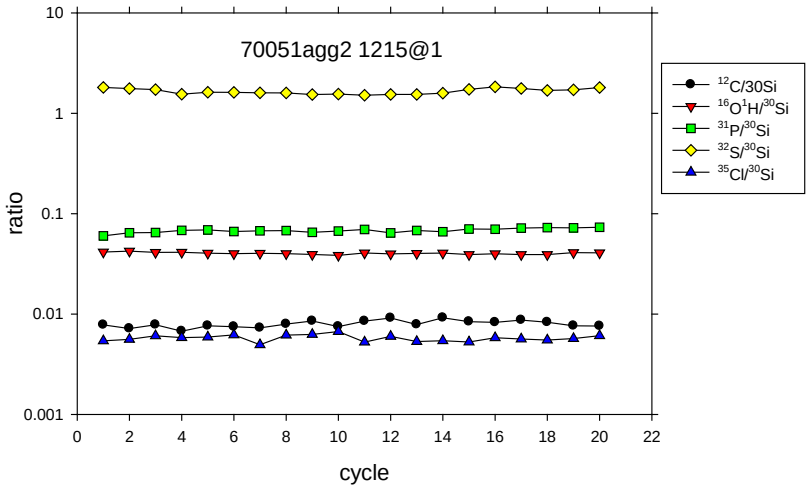

Time lapse for spot 1215@1

70051agg2ir

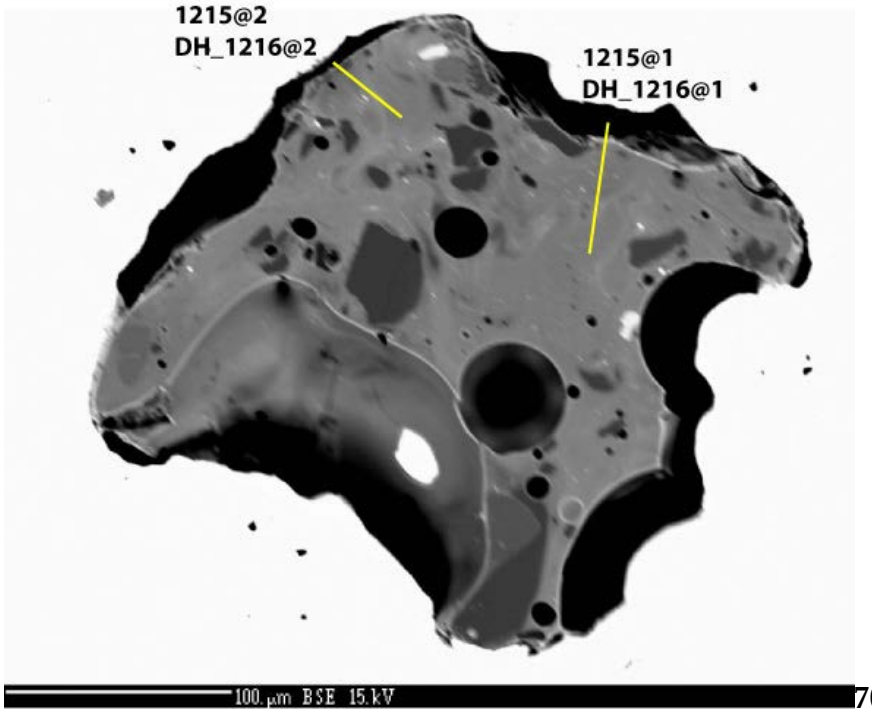

70051agg3ir

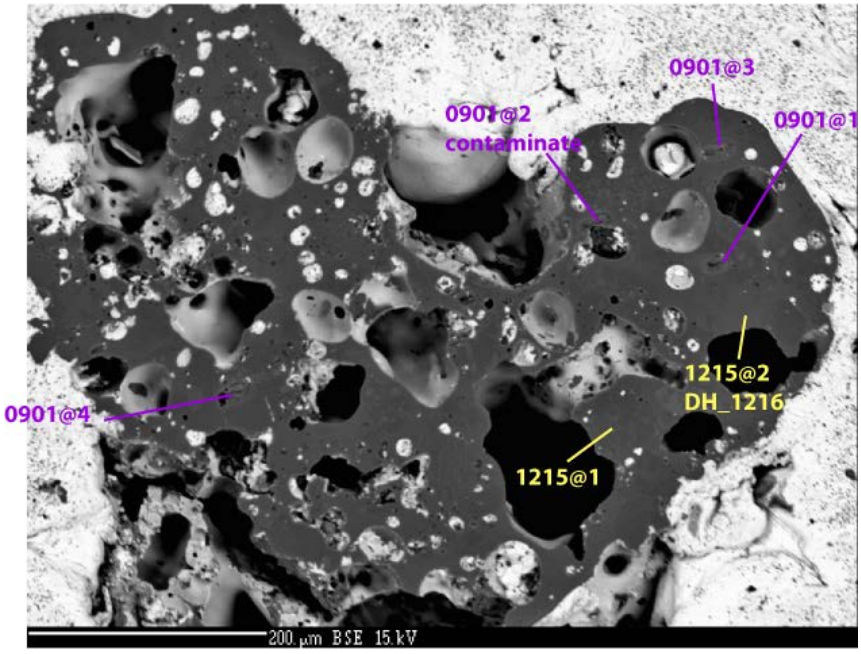

64051 agg3

Supplementary Figure 5. Measured versus modeled D/H values. The modeled D/H assumes all H was derived by solar-wind protons and D was from spallation. The large uncertainties in δD_{model} are due to the uncertainties in H contents.

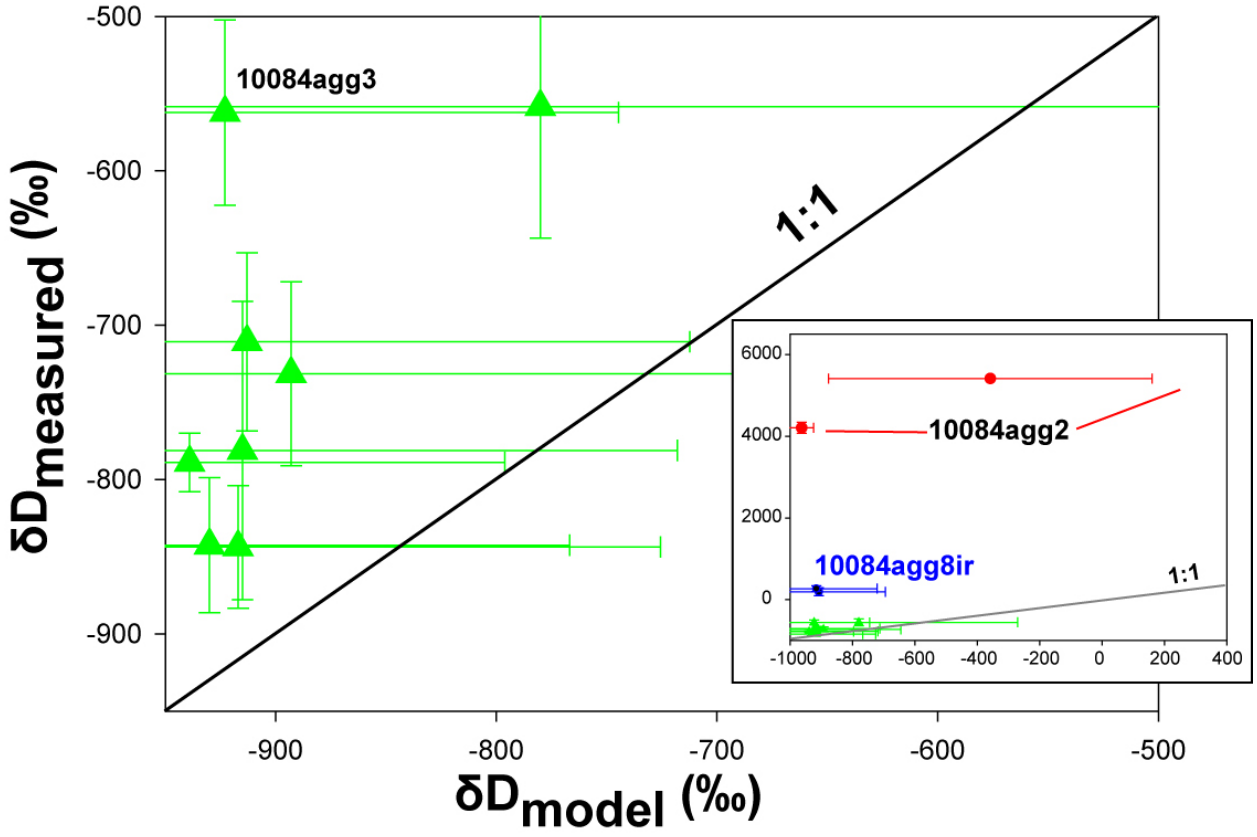

Supplementary Table 1. Composition of agglutinates and their OH contents (in ppmw H_2O).

sample	spot #	H_2O FTIR	H_2O SIMS	2σ	δD (‰)	2σ	P_2O_5	1σ	SiO_2	1σ	TiO_2	1σ	Al_2O_3	1σ	Cr_2O_3	1σ	MgO	1σ	CaO	1σ	MnO	1σ	FeO	1σ	Na_2O	1σ	K_2O	1σ	S	1σ	Total
impact glasses																															
10084impg1			<d.l.		nd		0.29	0.02	42.4	0.2	7.14	0.12	12.8	0.2	0.38	0.02	9.55	0.11	10.9	0.1	0.20	0.02	15.0	0.3	0.44	0.03	0.15	0.03	0.12	0.09	99.5
10084impg2			<d.l.		nd		0.27	0.03	42.2	0.2	7.28	0.14	12.7	0.1	0.39	0.03	9.91	0.09	10.7	0.1	0.21	0.02	15.0	0.3	0.45	0.02	0.14	0.04	0.34	0.46	99.6
70051b1			<d.l.		nd		0.08	0.03	38.4	0.1	9.27	0.17	5.69	0.06	0.68	0.05	14.8	0.1	7.16	0.09	0.28	0.02	22.6	0.2	0.34	0.01	0.06	0.03	0.12	0.15	99.4
64501gg			<d.l.		nd		0.19	0.02	44.5	0.2	0.48	0.08	26.9	0.2	0.11	0.02	7.00	0.14	15.2	0.2	0.07	0.02	5.20	0.16	0.22	0.10	0.06	0.01	0.26	0.28	100.1
agglutinates																															
Apollo 11 soil 10084																															
10084agg1ir	1215@2		187	40			0.23		43.9		2.58		20.3		0.18		7.5		13		0.13		11.5		0.34		0.05		0.01		99.6
10084agg2	0901@1		470	18	4555[2]	95[2]	0.21	0.03	42.1	1.9	6.47	2.2	13.4	2.9	0.29	0.09	9.23	0.71	12.2	0.4	0.22	0	15.0	2.2	0.41	0.08	0.09	0.01	0.43	0.24	100.1
10084agg2	1216_ DH		nd		4206	134																									
10084agg2	0901@2		27	14	5413[2]	687	0.35	0.03	41.0	0.3	10.8	0.3	9.52	0.15	0.32	0.06	6.8	1.3	10.7	0.6	0.25	0.02	19.7	1.4	0.53	0.07	0.17	0.03	0.47	0.46	100.6
10084agg2	0901_ DH@1		nd		1016[2]	32[2]	0.18		45.3		1.91		21.1		0.13		8.2		13.9		0.14		8.66		0.64				0.64		101
10084agg2	1216_ DH@1		nd		1372	142																									
10084agg3	0830@3		121	20			0.22	0.04	43.8	1.4	5.84	0.54	12.1	1.3	0.33	0.04	8.85	0.64	12.2	0.7	0.21	0.03	15.0	0.8	0.34	0.06	0.11	0.01	0.33	0.26	99.2
10084agg3	0830@4		*600*	*18*			0.39		41.2		10.7		9.65		0.44		8.60		11.6		0.23		16.9		0.43				0.25		100.4
10084agg3	0901@2		389	16			0.21	0.06	42.1	0.8	6.70	0.18	14.2	0.4	0.30	0.03	8.20	0.21	12.1	0.5	0.21	0.03	14.8	0.8	0.35	0.06	0.07	0.01	0.68	0.85	99.9
10084agg3	1216@1		316	40																											
10084agg3	1216@2		225	40	-562	60	0.26		42.2		6.63		15.2		0.26		8.09		12.3		0.19		14.3		0.43		0.17		0.13		100
10084agg4n	1215@1		177	40			0.22	0.01	40.7	0.7	7.67	0.2	15.4	1.3	0.31	0.04	7.46	0.59	12.2	0.2	0.19	0	15.1	0.3	0.41	0.03	0.10	0.02	0.10	0.00	99.9
10084agg4n	1215@2		282	40	-789	19	0.28		39.8		8.21		12.7		0.29		8.23		11.6		0.18		18.7		0.38		0.15		0.17		101
10084agg4n	1215@3		246	40	-843	44	0.23		43.2		6.64		9.43		0.36		10.4		12.3		0.23		16.4		0.30		0.09		0.06		99.6
10084agg5ir	0830@2		94	18			0.23		45.3		6.18		9.68		0.54		12.5		12.9		0.20		13.1		0.19				0.00		100.8
10084agg5ir	0830@3		61	16			0.25	0.06	42.0	0.0	8.13	0.04	13.0	1.0	0.27	0.14	7.59	2.08	11.7	0.1	0.23	0.01	17.2	1.2	0.27	0.00			0.19	0.27	100.8
10084agg5ir	0830@3b		293	26																											

10084agg5ir	0830@4		72	14			0.26		41.7		8.00		14.7		0.23		7.50		11.8		0.21		15.3		0.51				0.74		101.0
10084agg5ir	0831@1		48	14			0.25	0.02	42.9	0.8	7.55	0.71	14.6	2.0	0.28	0.09	7.63	0.32	13.1	0.9	0.17	0.1	13.2	3.7	0.57	0.24			0.30	0.26	100.5
10084agg6ir	1215@1	130	161	40	-731	60	0.25	0.07	41.5	0.8	8.09	0.7	12.8	0.3	0.31	0.01	7.95	0.08	11.6	0.2	0.20	0.00	16.8	1.9	0.42	0.03	0.12	0.04	0.13	0.10	100
		170																													
10084agg7	1215@1		83	40			0.20	0.02	42.2	0.3	7.52	0.2	12.7	0.1	0.29	0.00	8.90	0.12	11.6	0.0	0.22	0.00	15.2	0.0	0.52	0.04	0.06	0.03	0.26	0.06	99.6
10084agg7	1215@2		131	40			0.22		41.3		7.70		13.4		0.26		8.59		11.6		0.19		15.3		0.56		0.09		0.20		99.4
10084agg8	1215@1		188	40	191	99	0.20		41.5		9.11		11.3		0.27		8.27		11.6		0.21		16.8		0.49		0.08		0.23		99.9
10084agg8	1215@2		207	40	267	74	0.20	0.01	41.6	0.2	8.08	0.92	12.8	1.5	0.29	0.03	8.49	0.17	11.5	0.2	0.20	0.01	15.9	1.1	0.52	0.05	0.09	0.02	0.22	0.03	99.9
10084agg9	1215@3		47	40			0.54		54.1		1.35		16.3		<d.l.		1.27		8.99		0.17		14.1		1.44		0.75		0.07		99.2
10084agg9	1215@4		219	40			0.23	0.00	43.3	1.3	6.51	0.72	11.5	1.4	0.28	0.06	8.70	1.16	12.2	0.71	0.21	0.03	16.3	1.0	0.38	0.06	0.12	0.09	0.06	0.02	99.7
10084agg10	1215@2		49	40			0.46		53.1		1.94		16.7		0.03		1.82		9.52		0.15		13.9		1.41		0.78		0.12		99.9
10084agg10	1215@4		175	40			0.31		43.8		7.40		10.8		0.28		8.68		11.0		0.21		16.1		0.29		0.31		0.25		99.5
Apollo 17 soil 70051																															
70051agg2ir	0830@1		87	14			0.11		49.8		3.17		3.44		0.46		15.0		15.0		0.18		13.0		0.16						100.3
70051agg2ir	0831@1	150	171	14			0.14	0.03	38.9	0.8	6.84	0.32	14.0	0.6	0.41	0.06	10.1	0.4	10.8	0.3	0.19	0.02	17.8	0.5	0.22	0.03	0.06	0.00	0.46	0.44	99.9
70051agg2ir	0831@2		161	16			0.12	0.01	38.5	0.2	7.02	0.15	13.3	0.6	0.41	0.01	10.4	0.3	10.7	0.3	0.20	0.01	18.3	0.3	0.20	0.04			0.52	0.67	99.6
70051agg2ir	0831@3		154	16			*0.14*		*44.0*		*5.05*		*10.5*		*0.52*		*11.9*		*14.1*		*0.17*		*13.2*		*0.16*				*0.61*		*100.4*
70051agg2ir	1215@1	120	200	40	-711	58	0.15	0.03	38.2	0.4	6.89	0.16	13.9	0.2	0.42	0.05	10.0	0.23	11.0	0.1	0.19	0.02	18.3	0.7	0.22	0.02	<d.l.	0.03	0.40	0.41	99.7
70051agg3ir	1215@1	90	209	40	-844	40	0.19		41.3		7.30		12.0		0.36		9.43		13.5		0.22		15.3		0.39		<d.l.		0.08		100
70051agg3ir	1215@2	70	203	40	-781	97	0.15		40.6		8.12		12.4		0.40		9.94		11.3		0.22		16.4		0.38		0.06		<d.l.		100.0
Apollo 16 soil 64501																															
64501agg3	0901@3		203	16			0.23	0.01	43.5	0.9	0.92	0.14	27.0	1.2	0.11	0.02	7.38	1.18	15.5	0.4	0.08	0.03	5.25	0.53	0.40	0.07			0.23	0.12	100.3
64501agg3	0901@4		269	50			0.23	0.00	44.2	0.4	0.30	0.26	35.4	0.2			0.10	0.06	18.9	0.4	<d.l.		0.23	0.01	0.60	0.22			0.44	0.27	100.5
64501agg3	1215@2		79	40	-558	85	0.17		44.2		0.14		27.7		0.06		6.55		16.0		0.07		4.15		0.47				<d.l.		99.5
Mineral fragments in agglutinates[3]																															
10084agg1ir	1215@1	pl	<d.l.				0.29		43.4		<d.l.		36.2		<d.l.		0.05		20.0		<d.l.		0.19		0.36		<d.l.		<d.l.		100
10084agg3	0830@1	pl	*43*	*14*			0.22	0.03	44.4	0.3	0.42	0.18	30.5	0.9	0.05	0.02	3.68	0.59	17.4	0.3	<d.l.		3.17	0.48	0.47	0.03			0.13	0.24	100.4

	DH_plag@1				*2018*	*351*																							
10084agg5ir	0830@1	px	<d.l.				0.19	0.07	47.9	0.6	4.19	0.46	4.50	0.68	0.78	0.03	14.8	0.0	16.5	0.3	0.24	0.02	10.9	0.2	0.12	0.01		0.16	0.22	100.3
10084agg8	1215@3	pl	*15*	*40*	*952*	*208*	0.22	0.01	43.8	0.0	0.07	0.01	35.7	0.1			0.17	0.02	19.8	0.0	<d.l.		0.37	0.10	0.35	0.02	<d.l.	0.08	0.05	100.6
10084agg9	1215@2	px	<d.l.				0.12		51.7		0.87		1.04		0.27		18.7		6.21		0.37		21.8		<d.l.		<d.l.	<d.l.		101.1
10084agg10	1215@1	px	<d.l.				0.23	0.01	48.5	0.6	3.34	0.2	3.89	0.50	0.74	0.11	14.9	0.8	17.9	0.7	0.19	0.01	10.4	0.28	0.11	0.02	<d.l.	<d.l.		100.4
64501agg3	0901@1	ol	*46*	*14*			0.09		38.8		0.37		1.80		0.05		36.1		1.11		0.20		22.7		<d.l.			<d.l.		101.2
64501agg3	1215@1	px	<d.l.				0.16		44.0		0.44		20.9		0.12		11.9		11.8		0.15		13.0		0.35			0.24		103.1

[1]OH contents from FTIR were calculated using the OH band height at ~2350 cm-1 and a molar absorption coefficient of basaltic glass (Danyushevsky et al.[2]).

The 2σ uncertainties for SIMS measurements are based on repeated analyses of standards, fitting errors, and counting statistics. Italic numbers indicate possible terrestrial contaminations in the H abundances by SIMS because their vicinities to H hot spots (contaminates). The 1σ uncertainties for oxides are standard deviation of > 3 analyses near the same spots. d. l.: detection limit; nd, not determined.

[2] Errors of these D/H measurements are only from counting statistics.

[3] These D/H measurements on mineral fragments contain larger uncertainties than those from counting statistics owing to the low H contents in these minerals. pl: plagioclase; px: pyroxene; ol: olivine.